JGR Atmospheres

Increased Fire Activity in Alaska Since the 1980s: Evidence From an Ice Core-Derived Black Carbon Record

M. Roxana Sierra-Hernández[1] [ID]**, Emilie Beaudon[1]** [ID]**, Stacy E. Porter[1,2]** [ID]**, Ellen Mosley-Thompson[1,3]** [ID]**, and Lonnie G. Thompson[1,4]** [ID]

[1]Byrd Polar and Climate Research Center, The Ohio State University, Columbus, OH, USA, [2]Environmental Science Program, Wittenberg University, Springfield, OH, USA, [3]Department of Geography, The Ohio State University, Columbus, OH, USA, [4]School of Earth Sciences, The Ohio State University, Columbus, OH, USA

Abstract Wildfires emit large quantities of particles that affect Earth's climate and human health. Black carbon (BC), commonly known as soot, is directly emitted to the atmosphere by wildfires and other processes and can be transported and deposited in remote regions including high-altitude glaciers and the polar regions. Here, we present a continuous, high-resolution record of BC and ammonium (NH_4^+) from 1933 to 2001 extracted from two ice cores retrieved in 2002 from the col between Mt. Bona and Mt. Churchill in the Wrangell-St. Elias Mountain Range, southeast Alaska. Despite the substantial increase of BC from fossil fuels in the Arctic since the Industrial Revolution, BC at Bona-Churchill originates primarily from biomass burning and thus provides a record reflecting a fire history for Alaska. The BC record from Bona-Churchill reveals that high fire activity became more frequent after 1984 in agreement with Alaska fire records. Most years associated with high BC or high NH_4^+ before 1984 occurred during El Niño events when precipitation in Alaska was below "normal," suggesting that precipitation played an important role in modulating fire activity in Alaska prior to the 1980s. Conversely, years with high BC or NH_4^+ after 1984 coincided with years with "normal" and low precipitation, but elevated temperatures, strongly suggesting that temperature became a more dominant factor influencing fire activity in Alaska after the 1980s as suggested by other studies. Recent Alaska fire records and temperatures indicate that this trend has continued in the 21st century.

1. Introduction

Wildfires, one of the main natural disturbances in North American boreal forests, occur in Alaska every year between May and August. However, it is the sporadic large fires, ignited by lightning in remote areas, that shape the landscape of the Alaskan boreal forests (DeWilde and Chapin III, 2006; Kasischke et al., 2010, 2013; Macias Fauria & Johnson, 2008). The fire regime in Alaska is naturally regulated by climate, and by the structure of its ecosystems. However, it has been modified by human activities (human-caused fires, land management practices, and fire suppression policies) and by climate change (Chapin III et al., 2008; Kasischke et al., 2010; Partain et al., 2016; Todd & Jewkes, 2006; Young et al., 2017). In Alaska, the likelihood of large fires has increased since the 1980s (York et al., 2020), with the two largest fire years on record in 2004 and 2015, when 2.7 and 2.1 million hectares (ha) burned, respectively (AICC, 2020). An assessment of the 2015 fire season determined that anthropogenic climate change increased the risk of experiencing a severe fire season by 34%–60% (Partain et al., 2016). Recently, due to climate change, fire seasons in Alaska have become longer and warmer, thus providing time for more ignitions to occur and for small fires to grow into larger ones (Kasischke et al., 2010). Additionally, with the higher air temperatures, duff layers dry out more rapidly becoming more readily available as a fuel (Hu et al., 2015; York et al., 2020; Young et al., 2017).

Biomass burning, which refers to the burning of living and dead vegetation (e.g., forests, grassland, agricultural waste, wood) emits gases and aerosols that affect climate, air quality, and human health. Black carbon (BC), commonly known as "soot," is a carbonaceous material emitted by the incomplete combustion of carbon-based fuels (e.g., biomass, fossil fuels, biofuels). It is directly emitted to the atmosphere by anthropogenic and natural combustion processes such as the burning of fossil fuels for energy use, open fires in forests and savannas, and waste burning. Black carbon is refractory and water insoluble. It forms aggregates, and strongly absorbs radiation in the visible range, thus creating a positive radiative forcing on climate (Bond et al., 2007, 2013). Black carbon also affects human health and has been associated with respiratory and cardiovascular diseases and premature death (Niranjan & Thakur, 2017; Reid et al., 2016).

Black carbon particles, mostly emitted as hydrophobic particles, are removed from the atmosphere primarily by wet deposition. As BC particles age in the atmosphere, they become hydrophilic through condensation of soluble species (e.g., sulfuric and nitric acid) onto their surface, coagulation with other soluble species, and oxidation (Bond et al., 2013; Lund & Berntsen, 2012; Lund et al., 2017). The atmospheric lifetime of BC varies regionally and seasonally, roughly averaging 7 days (Bond et al., 2013; Cooke et al., 1999) depending on the aging process (e.g., soluble species concentrations, atmospheric conditions; Lund & Berntsen, 2012; Lund et al., 2017; Qi & Wang, 2019a; Zhang et al., 2019). Thus, BC particles can be transported over regional to intercontinental distances and deposited in remote regions including high-altitude glaciers and the polar regions. BC particles deposited on snow and ice can consequently accelerate cryospheric melting by reducing its albedo and increasing surface absorption of solar radiation (Bond et al., 2013).

Emission inventories confirm that since the onset of the Industrial Revolution ~1850, atmospheric BC emissions have risen considerably worldwide, although with regional variability, largely due to fossil fuels combustion and biomass burning associated with widespread deforestation (Bond et al., 2007, 2013). Unfortunately, these emission inventories contain large and significant uncertainties as they do not account for rapid changes such as wars or economic depressions and may vary regionally yielding incorrect spatial distributions (Bond et al., 2007). Thus, while atmospheric measurements are needed to better quantify current BC emissions, natural archives are also necessary to reconstruct historical emissions.

Ice cores are natural archives exclusively fed by atmospheric input and can provide more detailed information including broader spatial and longer temporal histories of BC deposition in remote regions compared to other natural archives (e.g., tree rings, lake sediments, and peat bogs). There are a number of ice core records of BC from different regions including Greenland (McConnell et al., 2007) and Svalbard (Osmont et al., 2018; Ruppel et al., 2014) in the Arctic, the Canadian high-Arctic (Zdanowicz et al., 2018) and sub-Arctic (Mt. Logan; Menking, 2013), Washington State in North America (Kaspari et al., 2020), western and eastern Europe (Lim et al., 2017; Sigl et al., 2018), Tibet and the Himalayas (Barker et al., 2021; Kaspari et al., 2011; Wang et al., 2015), and Antarctica in the Southern Hemisphere (Bisiaux et al., 2012). In most of these existing BC ice core records, anthropogenic activities were the primary source of BC depositions during the 20th century.

Here, we present a record of BC between 1933 and 2001 from an ice core retrieved in 2002 from the col between Mt. Bona and Mt. Churchill in the Wrangell-St. Elias Mountain Range, southeast Alaska (61.4°N; 141.7°W; 4,420 masl; Figure 1). Since anthropogenic BC emissions increased worldwide primarily during the 20th century, we take advantage of the high-resolution BC ice core record from Bona-Churchill, to explore possible contributions from anthropogenic and natural sources deposited in this region. To overcome the possible impact of anthropogenic sources in the BC record, a record of NH_4^+ from an ice core extracted in close proximity to the BC ice core is also used as concomitant increases of BC and NH_4^+ are associated with forest fires (Keegan et al., 2014; Legrand et al., 2016). The Bona-Churchill ice core records are then compared with the documented Alaska fire history, and with temperature, precipitation, and El Niño events to determine their influence on the BC and NH_4^+ signals recorded at Bona-Churchill. To assess regional variability, comparisons are also made with other existing regional ice core records of different biomass burning proxies: (a) levoglucosan, and dehydroabietic and vanillic acids from Aurora Peak at 2,825 m asl, northwest of Bona-Churchill, which recorded forest fires from Alaska and Siberia (Pokhrel et al., 2020); (b) NH_4^+ from Mt. Logan at 5,340 m asl, ~150 km southeast of Bona-Churchill and closer to the coast, which appears to have recorded primarily more distant forest fires in Siberia (Whitlow et al., 1994); and (c) NH_4^+ from the Eclipse Icefield just 45 km northeast of Mt. Logan at 3,017 m asl which recorded primarily regional forest fires from Alaska and the Yukon Territory (Yalcin et al., 2006). Given Bona-Churchill's different elevation and coastal influence, its BC and NH_4^+ ice core-derived records will provide new information of forest fire activity and climate variability in Alaska. In addition, this study uses two biomass burning proxies, BC and NH_4^+, which have not been reported together in other ice cores from this region.

2. Methodology

2.1. Bona-Churchill Ice Cores

In the spring of 2002, six ice cores (two deep and four shallow ice cores) were drilled from the ice field covering the Bona-Churchill col. The two deep cores used for this study were drilled ~200 m apart (Urmann, 2009). One was drilled 460.96 m to bedrock (B-Ch1) and the second (B-Ch2) was drilled to ~118 m depth (Porter

Figure 1. Map of Alaska showing the locations of the drilling sites of the Bona-Churchill (black star) ice cores, and the Eclipse (1), Mt. Logan (2), and Aurora Peak (3) ice cores. The cities of Anchorage, Fairbanks, and Tok that connect the most important transportation routes are also shown. The Kenai National Wildlife Refuge (south of Anchorage) is outlined for reference. Cluster means of 3-day back trajectories between 1948 and 2001 for May–August (see text for details) are also displayed with the percentage of trajectories allocated to each cluster.

et al., 2019; Urmann, 2009). While some thin melt layers of ~1 mm were present throughout both cores, no indications of seasonal melt were evident (Porter et al., 2019).

The time scale was reconstructed from B-Ch1 by annual layer counting of the concentrations of insoluble dust particles that peak during spring such that annual layers roughly approximate the thermal year (July–June). The time scale was verified by high beta radioactivity from atmospheric thermonuclear testing detected in the 1963 dust peak at 78 m depth and by multiple volcanic markers such as the Katmai eruption in 1912 (Porter et al., 2019). For details on the analyses of dust particles and beta radioactivity, the reader is referred to Urmann (2009). A time scale was obtained for B-Ch2 by matching the $\delta^{18}O$ of B-Ch2 with that of B-Ch1. For this study, and to facilitate comparison among data sets and inventories, the time scales were converted to calendar year.

2.2. Sample Preparation and BC Analysis

Black carbon measurements were performed on the entire B-Ch2. The ice core was sampled continuously at sub-annual resolution over the entire record (6–30 samples year^{-1}) producing a total of 1,172 samples with a sample size of 10–15 cm for the top 5 m, and of 8–10 cm below 5 m. Samples that originate from the top 69 m of B-Ch2, consisting of consolidated firn, were cut with a bandsaw as follows. An artificial ice core made of ultrapure (UP)

water (18.2 MΩ) was used to clean the bandsaw before a thin slab of 1 cm thickness was cut from the ice core surface and used to hold an inner second slab also of about 1 cm thickness, which was never in contact with the bandsaw surface or guide. Firn samples were handled using triple-rinsed gloves and immediately placed in individual clean, heat-sealed polyethylene (PE) bags. Ice samples below 69 m were cut with the same bandsaw after removing an outer 0.5 cm thick slab. Ice samples were rinsed with UP water in a class 100 clean room to remove any possible contamination and were immediately placed in individual clean heat-sealed PE bags and stored frozen until further analysis.

The quantification of BC was performed in a class 100 clean room using a Single Particle Soot Photometer (SP2; Droplet Measurement Technologies, Longmont, USA). The SP2 directly measures only the refractory and strongly light-absorbing BC, specifically referred to as rBC in some publications; however, here we simply use BC. The energy emitted during incandescence is measured, and a quantitative determination of BC mass of the particle is made independently of its morphology and coating (Schwarz et al., 2006, 2012). An external calibration curve of five Aquadag standards (0.5–15 ng g^{-1}) was prepared daily and analyzed before the samples to correct for BC loss during nebulization (Wendl et al., 2014). Frozen firn and ice samples were melted at room temperature in their individual PE bags for about 20–30 min and immediately transferred into 50 mL polypropylene conical screw cap tubes (Sarstedt Inc.) minimizing potential BC particle loss (Barker et al., 2021; Wendl et al., 2014). Samples were then sonicated for at least 20 min and analyzed immediately. Samples were continuously stirred with a magnetic bar as they flowed into a CETAC Marin-5 enhanced nebulizer system (Teledyne CETAC Technologies, Omaha, USA) using a peristaltic pump. The nebulized sample was introduced to the SP2 sample inlet at a known rate using carbon-free air carrier gas. A UP water blank was analyzed every five samples to monitor the instrument baseline conditions. The baseline remained stable for all the B-Ch2 measurements as the core was very "clean" with low dust concentrations for B-Ch1 averaging $21 \times 10^3 \pm 9 \times 10^3$ particles (0.63–16 μm diameter) per milliliter between 1933 and 2001. Procedural blanks (UP water frozen as an artificial ice core) were cut, prepared, and analyzed similar to the firn and ice samples and they showed negligible BC concentrations (<0.1 ng g^{-1}). The limit of detection was determined as the average of 20 UP blanks plus 3SDs as 0.3 ng g^{-1}. The averaged analytical uncertainty is estimated to be $<10\%$. UP water was flushed through the system after all the daily sample measurements for at least 5 min or until stability was achieved. The SP2 output data were processed using the PSI SP2 Toolkit 4.200f (Paul Scherrer Institut, CH) and the IGOR Pro software platform (WaveMetrics Inc., Portland, USA).

2.3. Ammonium Analysis

The 1933–2001 ammonium (NH_4^+) record used here originates from the deep B-Ch1 ice core. The sample preparation and analysis of major anions and cations, including NH_4^+, were performed as described by Urmann (2009). Briefly, the ice core samples were transferred to a Class 100 clean room where they were rinsed with UP water and melted at room temperature before being analyzed for NH_4^+ and other major ions with a Dionex ICS-2500 ion chromatograph (for more details the reader is referred to Porter et al., 2019 and Urmann, 2009). Additionally, the top half of the B-Ch2 core (1973–2001), from which the BC record originates, was analyzed for major ions using a Thermo Scientific ICS-5000 ion chromatograph. The NH_4^+ records from both cores are significantly correlated ($\rho = 0.81$, $p < 0.01$, Figure S1 in Supporting Information S1) indicating that glaciological noise is negligible and thus, the 1933–2001 NH_4^+ record from B-Ch1 can be combined with that of BC from B-Ch2.

2.4. HYSPLIT

Using the PC version of HYSPLIT, 7-day back trajectories were calculated daily from May to August, which correspond to the fire season in Alaska, for the 1948–2001 period generating a set of 25,056 back trajectories to geographically constrain the atmospheric influence at Bona-Churchill. It should be noted that while the back trajectories were performed for the fire season in Alaska, BC and NH_4^+ from anthropogenic sources can be deposited in other seasons, for instance during late winter and spring when the Arctic haze occurs (Winiger et al., 2019). To better visualize flow patterns, back trajectories close to each other were merged into clusters by their mean trajectory using the HYSPLIT cluster analysis tool. To efficiently run the cluster analysis of this large set of back trajectories, only 72 h (3 days) and 120 h (5 days) trajectories were clustered using every hourly endpoint, and given the very large set of trajectories, a five-trajectory skip was used (the cluster tool only includes every fifth

trajectory of the data set). A similar cluster analysis was also performed for Eclipse, Mt. Logan, and Aurora Peak trajectories.

2.5. Alaska Fire History

Historical fire records provided by the Alaska Interagency Coordination Center (AICC), Bureau of Land Management (BLM; AICC, 2020), comprise total area burned, number of fires, and fire perimeters since 1939 when fire monitoring began in Alaska. This data set includes wildfires across Alaska that occurred naturally (e.g., lightning) or anthropogenically, either accidentally (e.g., escaped campfire) or intentionally. To reconstruct the Alaska fire history for the 1939–1970 period, the agency personnel used archival fire records, letters, reports, and other unpublished documents. After 1980, satellites, more remote automatic weather station data, and other technological advancements facilitated the detection, monitoring, and suppression of fires which improved the quality of the Alaska fire data set post-1980s. Thus, although the data set is comprehensive and up-to-date, it is not complete, and it continues to change as new information prior to the 1980s is located (Kasischke et al., 2002; Todd & Jewkes, 2006). Here, we use the total area burned (Table S1 in Supporting Information S1) for comparisons with the BC and NH_4^+ records from Bona-Churchill.

2.6. Energy Consumption and Black Carbon Emissions

To explore the possible emission sources of the observed black carbon, the Bona-Churchill ice core record is compared with inventories of energy consumption and black carbon emissions.

2.6.1. Energy Consumption

The energy consumption in Alaska is obtained from the U.S. Energy Information Administration (EIA, 2019) by energy source (e.g., fossil fuels, biomass, renewables, etc.). Since wood is an important energy source in Alaska for residential heating and a source of black carbon, here in addition to fossil fuel consumption, we use biomass (wood and wood waste) consumption to compare the changes in trends with the Bona-Churchill ice core record.

2.6.2. Black Carbon Emissions

Unfortunately, BC emission estimates for Alaska are unavailable for the period of study here. Thus, annual BC emission grid maps ($0.1° \times 0.1°$) from the Emissions Database for Global Atmospheric Research (EDGARv5.0; Crippa et al., 2019; EDGARv5.0, 2020) are used to construct a time series of anthropogenic BC emissions for Alaska. It is important to note that EDGARv5.0 does not include emissions from large-scale biomass burning (e.g., savannah burning, forest fires). Also, BC emissions are distributed using spatial data such as population density, land use, road network, animal density, inland waterways, and aviation and international shipping routes (Greet et al., 2013) which can introduce large uncertainty. In addition to the BC emission estimates for Alaska, we use BC emissions estimates for the United States and East Asia reported by Bond et al. (2007) and Fernandes et al. (2007).

2.7. Black Carbon Deposition From MERRA-2

The Bona-Churchill BC data are compared with the Modern-Era Retrospective Analysis for Research and Applications Version 2 (MERRA-2) reanalysis data provided for this study by the Global Modeling and Assimilation Office, NASA/Goddard Space Flight Center. MERRA-2 provides data beginning in 1980 at an approximate resolution of $0.5° \times 0.625°$ with 72 vertical levels up to 0.01 hPa (Gelaro et al., 2017; Randles et al., 2017). Carbonaceous aerosol emissions in MERRA-2 coupled with the Goddard Chemistry, Aerosol, Radiation, and Transport (GOCART) model include natural and anthropogenic sources derived from several emission inventories. It should be noted that although MERRA-2 often overestimates BC at higher altitudes, airborne measurements from the Arctic suggest MERRA-2 underestimates BC in the northern high latitudes (Randles et al., 2016). All aerosols are subject to dry deposition, wet removal, and convective scavenging. Wet deposition of the aerosols depends on precipitation which is corrected using observations to reduce errors (Randles et al., 2017).
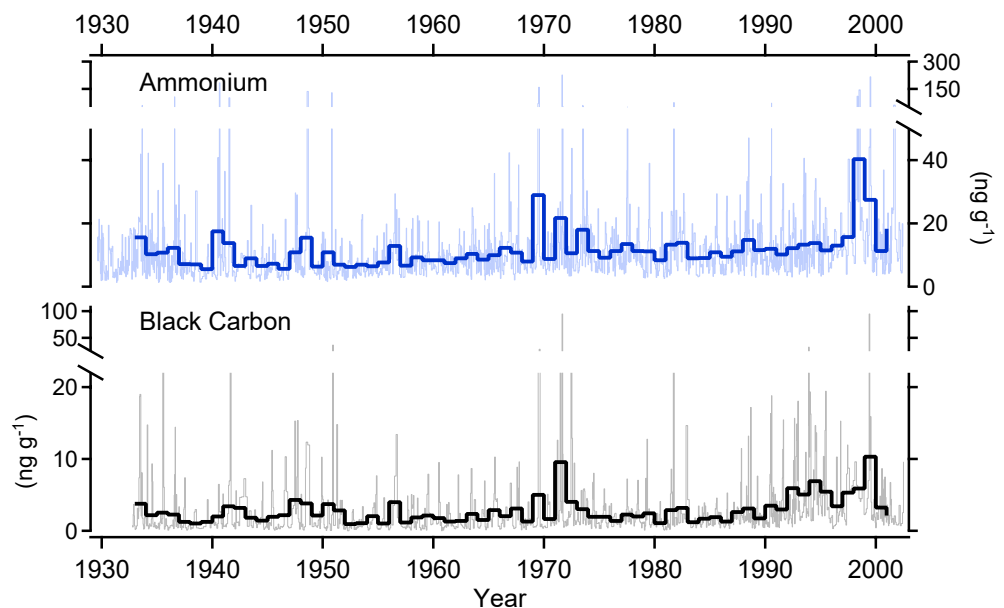
Figure 2. Black carbon and NH_4^+ concentrations between ~1930 and 2001. The thin lines represent the individual sample concentrations and the thick lines reflect their respective annual averages.

2.8. Climate Data

Summer (June–August, corresponding to the peak of the fire season) precipitation and temperature for Alaska were obtained from the NOAA National Centers for Environmental Information, Climate at a Glance (NOAA, 2020a) for the period 1925–2020. El Niño 3.4 sea surface temperature anomalies were obtained from NOAA ESRL Physical Sciences Laboratory website (NOAA, 2020b). In the supporting information, atmospheric circulation patterns were explored for two high fire years using NCEP/NCAR reanalysis (Kalnay et al., 1996).

Following the reporting method used in the NOAA Arctic Report Card 2020 (York et al., 2020), total area burned, summer precipitation in Alaska, and the Bona-Churchill BC and NH_4^+ annual fluxes are distributed in terciles. To be consistent with the correlations among the different climate variables, the terciles are determined based on the entire timespan contained in the Bona-Churchill ice core record (1939–2001). For a particular variable, a year is considered to be "normal" when the variable falls within the second tercile (33rd–66th percentile of the 1939–2001 distribution), and below or above "normal" when it falls within the first tercile (<33rd percentile of the 1939–2001 distribution), and the third tercile (>66th percentile of the 1939–2001 distribution), respectively. For instance, years with >270,000 ha burned are considered large fire years, and summers with precipitation <24 cm are considered low precipitation summers or dry years. It is important to note that there are spatial variations in the precipitation data that are not accounted for here.

2.9. Statistical Analysis

All statistical analyses including averages, factor analysis of the ranked data, cluster analysis, and Mann-Kendall trend test were performed using Minitab 18, while the terciles, nonparametric Spearman-ranked correlations (correlation coefficient ρ), and sequential Mann-Kendall test (Dey, 2021) were obtained with MATLAB 2020 and 2021.

3. Results and Discussion

The BC and NH_4^+ concentration time series are shown in Figure 2. To understand the role of NH_4^+ and identify its possible sources in the Bona-Churchill ice core record we first applied a multivariate factor analysis to the full ion and dust data set from B-Ch1 between 1930 and 2001. It was not possible to include BC in the factor analysis as it comes from the B-Ch2 core with a different sampling resolution. Four factors, explaining 85% of the total
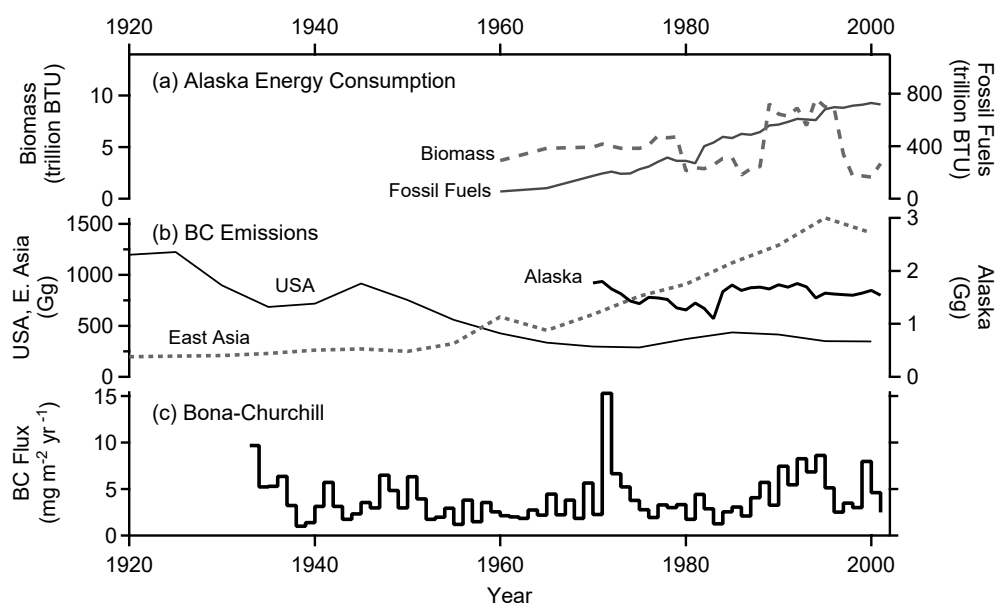
Figure 3. Comparison of (a) annual energy consumption of biomass (dotted line), and fossil fuels (solid line) in Alaska (EIA, 2019), (b) annual BC emissions from human activities (not including wildfires) from the EDGARv5.0 database for Alaska (Crippa et al., 2018, 2019; EDGARv5.0, 2020), and for the United States and East Asia region (Bond et al., 2007; Fernandes et al., 2007), and (c) the Bona-Churchill ice core-derived black carbon flux record for comparison. Note the left and right axes are different in panels (a) and (b).

variance were extracted from the data, and a cluster analysis of these four factors was also performed to group the ions and dust particles into clusters that share common characteristics or sources. Factor 1 (29% variance) is loaded in Mg^{2+}, Ca^{2+}, and dust particles which are of crustal origin. Factor 2 (21% variance) is loaded in Cl^- and Na^+ suggesting a marine origin. Factor 3 explains 18% of the variance and is loaded in NO_3^- and SO_4^{2-} which are likely of anthropogenic origin. The NH_4^+ and K^+ are grouped together in Factor 4 (17% variance) and likely share common sources including biomass burning which suggests that NH_4^+ in the Bona-Churchill ice core could be used as a reliable proxy of biomass burning in the region.

Despite coming from different cores, annual BC and NH_4^+ concentrations are significantly correlated ($\rho = 0.70$, $p < 0.001$, Figure S2 in Supporting Information S1) demonstrating reproducibility between B-Ch1 and B-Ch2 and also suggesting common sources. Other studies in ice cores have demonstrated that the source of concomitant increases of NH_4^+ and BC are large forest fires (Keegan et al., 2014; Legrand et al., 2016). Legrand et al. (2016) also found a strong correlation between BC and NH_4^+ in Greenland ice cores tracing past boreal forest fires. BC and NH_4^+ have been considered reliable proxies of forest fires in ice cores from Greenland, along with other species including organic carbon, and formic and vanillic acid (Legrand et al., 2016). However, BC emissions from fossil fuel combustion have increased considerably since 1850 (Bond et al., 2007) and have affected BC trends in ice core records from Greenland (McConnell et al., 2007), and other Arctic sites (Osmont et al., 2018; Ruppel et al., 2014; Zdanowicz et al., 2018). Contrary to Greenland, in the Canadian sub-Arctic, it was estimated that between 2007 and 2013, biomass burning contributed 59%–78% of annual BC during summer and 28%–32% during winter (Qi & Wang, 2019a). BC then must be used with caution when using it as a proxy of biomass burning after 1850. Thus, it is important to first determine the possible impact of fossil fuel and biofuel combustion sources of BC in the Bona-Churchill ice core.

3.1. Anthropogenic Sources

Unfortunately, no direct source apportionment data are available for anthropogenic sources of BC, therefore only available energy consumption and BC emission inventories are used here for qualitative comparisons (changes in trends) to determine the possible contribution of anthropogenic sources to the BC deposited at Bona-Churchill. For this, we first compare the energy consumption (fossil fuels and biomass) in Alaska since 1960 (Figure 3a),

the BC emissions from Alaska since 1970, and from the United States and East Asia since 1920 (Figure 3b) with the BC ice core record (Figure 3c).

In Alaska, fossil fuel consumption has been continuously increasing from ∼50 million BTU since 1960 to ∼730 million BTU in 2001 (Figure 3a). Biomass consumption, about two orders of magnitude lower than fossil fuel consumption, has varied over time with two periods of low consumption (∼2 million BTU) in 1980–1990 and in 2000 (Figure 3a). On the other hand, anthropogenic BC emissions in the United States increased considerably since the Industrial Revolution in the late 1850s (not shown) until ∼1925 after which they have been intermittently decreasing as a result of the Great Depression in the 1930s and the introduction of the Clean Air Act in 1970 (Bond et al., 2007; Fernandes et al., 2007). Additionally, BC emissions in Alaska (Figure 3b) reflect a decreasing trend between 1970 when the EDGARv5.0 record begins, and the early 1980s, in accordance with the inventory from Bond et al. (2007). After 1982, BC emissions in Alaska likely increased as the result of a more rapid rise in the population and the construction of infrastructure such as the trans-Alaska pipeline, however, emissions remained below the 1970's level. These anthropogenic trends are reflected in the BC ice core records from Greenland (McConnell et al., 2007) but not in the Bona-Churchill BC record (Figure 3c). The Mann-Kendall trend test confirms that the trend in BC flux is not monotonic. To further corroborate that there is no increasing trend in the BC flux, a sequential Mann-Kendall test was performed to detect change points. Five change points were detected at years 1941 ($\alpha = 0.05$), 1962 ($\alpha = 0.05$), 1972 ($\alpha = 0.1$), 1984 ($\alpha = 0.1$), and 1995 ($\alpha = 0.1$) which do not correspond to any anthropogenic changes in emissions. These results strongly suggest that human activities are not a dominant source of BC in this region. To further determine the possible sources of BC at Bona-Churchill we examined the Bona-Churchill ice core record relative to fire-related data in the next section.

3.2. Forest Fires

Several events of concomitant high BC and high NH_4^+ are observed in the Bona-Churchill record: 1933–1936, 1941, 1948, 1950, 1965, 1969, 1971, 1973–1974, 1981, 1987–1988, during the 1990s, and in 2000 (Figure 2) with large forest fires as their likely source.

The MERRA-2 data show that BC is deposited at Bona-Churchill primarily between May and August, and deposition is dominated by wet deposition of aged BC (89.3%) and BC emissions from biomass burning (5.3%). Comparison of the BC from the B-Ch2 ice core with modeled BC deposition (Figure S3 in Supporting Information S1, 1980–2002) and with dust particles from B-Ch2 (Figure S4 in Supporting Information S1, showing the bottom of the record 1933–1950) reveal that the measured BC is deposited simultaneously with the modeled BC and with the dust particles during spring and summer, when forest fires are the primary source of BC in the Arctic and sub-Arctic (Hegg et al., 2010; Qi & Wang, 2019a, b; Winiger et al., 2019). Cluster analysis of 3-day back trajectories for the months of May–August shows that 28% of the air parcels reaching Bona-Churchill originate from the interior where boreal forest fires in Alaska predominantly occur (Figure 1). Thus, BC detected in the Bona-Churchill ice core very likely originates primarily from local and regional forest fires.

Between 1939 and 2001, the number of large fire years in Alaska varied from decade to decade with the lowest frequency in the 1950s and 1960s and the highest frequency in the 1990s. A similar trend is observed in the Bona-Churchill BC ice core record as shown in Figures 4 and 5. A low but significant correlation exists between the area burned in Alaska and the BC flux record between 1939 and 2001 ($\rho = 0.3$, $p = 0.02$). This is expected as atmospheric circulation in Alaska during the fire season is complex (Hayasaka et al., 2016) and thus, not all fires will be preserved in an ice core (see case study in Text S1 in Supporting Information S1). Despite the low correlation, 14 years of high BC or NH_4^+ coincide with 67% of Alaska's large fire years, including 1947 and 1969, when some of the largest fires occurred in the Kenai Peninsula (AICC, 2020; Anderson et al., 2006; De Volder, 1999), near and upwind of Bona-Churchill (Figures 1 and 4), suggesting that Bona-Churchill reflects the fire activity in Alaska which further indicates that BC originates primarily from forest fires.

3.2.1. Alaska Fire History and Climatology

Since the first fire control agency in Alaska was created in 1939, a wildfire suppression policy was implemented to suppress all fires. Fire suppression is a particularly challenging task in Alaska due to its climate, topography, and the vast interior area where most wildfires occur (Todd & Jewkes, 2006). However, the capabilities of fire agencies in Alaska have evolved and improved with time.
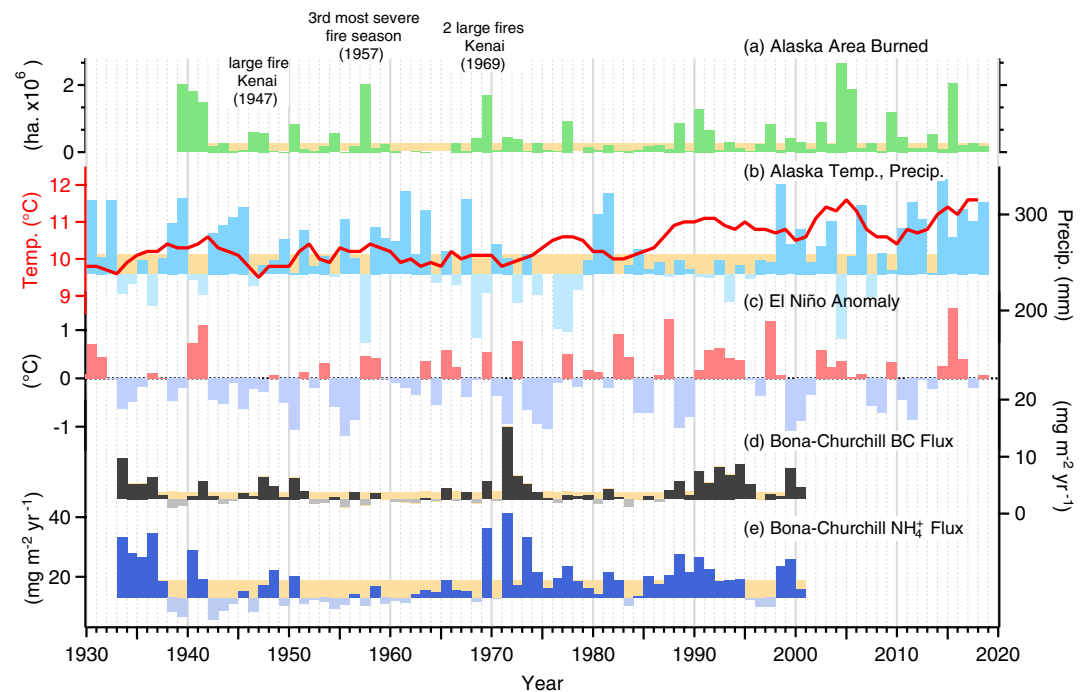
Figure 4. Comparison of (a) total area burned in Alaska (AICC, 2020), (b) summer temperature 5-year running average (red continuous line) and summer precipitation (NOAA, 2020a) in Alaska, (c) El Niño 3.4 anomaly (NOAA, 2020b; Rayner et al., 2003), and the Bona-Churchill annual (d) black carbon (BC), and (e) NH_4^+ fluxes. The shaded area is the middle tercile (33rd–66th percentile of the 1939–2001 distribution) which is considered "normal" for area burned, precipitation, and the Bona-Churchill BC and NH_4^+.

Initially, during the 1940s, fire suppression was very limited due to the lack of human and technological resources to detect and reach remote wildfires. Fire suppression improved during the 1950s and 1960s as more and better resources (e.g., aircraft, riverboats, smokejumpers, and chemical fire retardants) became available to the BLM Division of Forestry allowing them to reach remote wildfires (Todd & Jewkes, 2006). Coincidentally, between the 1950s and 1970s, the number of large fires, the annual area burned in Alaska, and the number of high BC and NH_4^+ years in the Bona-Churchill ice core record were low, with the lowest number of these fire characteristics occurring in the 1950s–1960s (Figures 4 and 5).
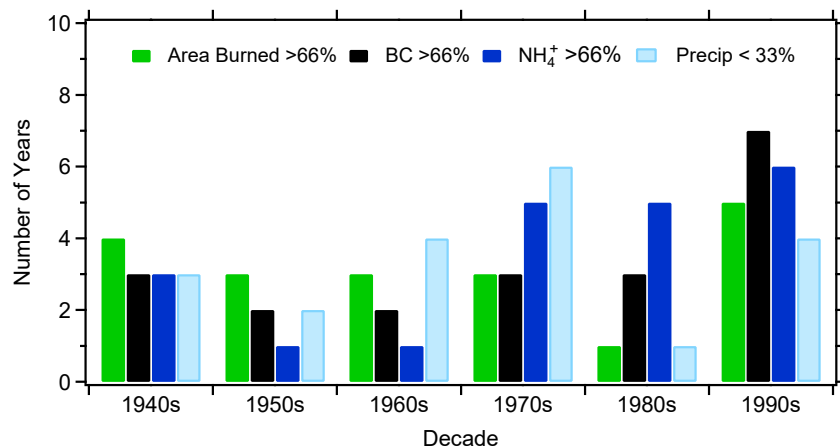

Figure 5. Number of years above "normal" (large fire years) per decade for total area burned in Alaska, Bona-Churchill BC and NH_4^+ annual fluxes, and below "normal" precipitation (dry years).

Table 1
Spearman Correlations Between Summer Precipitation, Summer Temperature and Black Carbon and Ammonium (NH_4^+) Fluxes From Bona-Churchill, and Area Burned in Alaska

Period	Precipitation			Temperature		
	Black carbon	NH_4^+	Area Burned	Black carbon	NH_4^+	Area Burned
Pre-1949[a]	**−0.7 (<0.01)**	**−0.7 (<0.01)**	−0.2 (0.48)	−0.1 (0.78)	0.0 (0.86)	0.6 (0.07)
1950–1977	0.0 (0.92)	−0.3(0.20)	**−0.6 (<0.01)**	0.0 (0.74)	−0.1 (0.91)	**0.5 (<0.01)**
1978–2001	−0.2 (0.40)	0.0 (0.90)	0.2 (0.45)	**0.6 (< 0.01)**	0.3 (0.23)	0.2 (0.2)
2002–2019	–	–	**−0.7 (<0.01)**	–	–	**0.7 (<0.01)**

Note. *p*-Values are shown in parentheses. Significant correlations (*p* < 0.05) are in bold.
[a]1933–1949 for Bona Churchill, and 1939–1949 for area burned in Alaska.

In 1982, the Alaska Interagency Fire Management Council changed its wildfire suppression policy from total fire suppression to fire management which designates four different levels of suppression. Areas where people and settlements are at risk receive the highest suppression priority and efforts, while in remote areas limited fires are generally allowed to burn (Todd & Jewkes, 2006). Coincidentally, since 1984 the number of large fires, the annual area burned in Alaska, and the number of years with high BC or high NH_4^+ in the Bona-Churchill ice core record increased to their highest levels in the 1990s (Figures 4 and 5).

It is possible that changes and improvements in fire suppression may have played a role in modifying the Alaskan fire regime, although this is debated. In a dendroclimatology study of a 250-year fire history in the Yukon Flats National Wildlife Refuge in interior Alaska (Drury & Grissom, 2008), the authors found no evidence that the changes in fire management policies influenced the fire regime in the Yukon Flats. Investigating the effect of human actions on fire regime, DeWilde and Chapin III (2006) found a 50% reduction in the proportion of burned areas designated with the highest level of suppression priority between 1992 and 2001, compared to areas designated as limited or without suppression in interior Alaska. Other studies have shown that Alaska's fire regime is driven primarily by climate and that large fires occur during unusually dry years (Duffy et al., 2005; Hess et al., 2001). Hess et al. (2001) showed that most of the large fires in Alaska occurred during moderate to strong El Niño events. During El Niño events, temperatures are typically near normal in western Alaska and often much warmer in southeastern Alaska (Hess et al., 2001; Nguyen et al., 2021; Papineau, 2001). In addition, Hess et al. (2001) argued that during El Niño events, precipitation increases along the coastal regions of Alaska and decreases further inland creating conditions that promote progressive drying of vegetation which favors more intense and widespread fires.

Temperature variations in Alaska during the 20th century show three distinct periods (Figure 4b) consistent with multidecadal variability in the Pacific: a warm period between 1920 and ~1950 with several years of high precipitation, followed by a cool and relatively wet period with some dry years mostly in the 1970s, and another warm period between ~1978 and 2000 with both dry and wet years (Bieniek et al., 2014). To better understand the role of temperature and precipitation in forest fires in Alaska and in the BC and NH_4^+ records in the Bona-Churchill ice core, correlations were performed between these two climate variables and the annual area burned in Alaska and the BC and NH_4^+ fluxes from Bona-Churchill (Table 1).

Precipitation negatively correlates with BC and NH_4^+ fluxes between 1933 and 1949 which suggests that these events may have resulted from low precipitation as shown in other studies (Duffy et al., 2005; Hess et al., 2001). Also, a weak negative correlation exists between precipitation and area burned for the 1939–1949 period. However, this correlation is not significant or meaningful due to the limited period of overlap (10 years) between the two records. For the 1950–1977 period, a significant negative correlation exists between precipitation and area burned suggesting that low precipitation influenced large fires during these periods of time. Even though no significant correlations exist between precipitation and BC or NH_4^+ during 1950–1977, high BC and high NH_4^+ years coincided with years of low precipitation (Figures 4b, 4d and 4e) indicating that low precipitation may have been a factor in these events. In fact, most of the pre-1978 large fire years in Alaska and most of the high BC and high NH_4^+ years in the Bona-Churchill ice core record occurred during years of low precipitation. Namely, the third largest fire on record in 1957 occurred during the year of lowest precipitation during the period of study. On

the other hand, between 1978 and 2001, 6 large fire years in Alaska and 9 years of high BC and high NH_4^+ in the Bona-Churchill ice core occurred during years of either "normal" or low precipitation (Figure 4). Thus, factors other than precipitation must have influenced the increase of large fires during this period of time.

Overall, temperatures in Alaska have increased ∼1°C between 1920 and 2012 (Bieniek et al., 2014) and ∼1.5°C by 2018 becoming particularly warm since the mid-1980s (Figure 4b). During this time, relatively warm conditions persisted in Alaska between 1920 and ∼1950 (Bieniek et al., 2014). The Alaska fire history does not cover the period prior to 1939 (Figure 4a) and Bona-Churchill coverage begins in 1933 (Figure 4d). Thus, we cannot fully determine the relationship between temperature and fire activity in Alaska during the entire 1920–1950 period. However, Bona-Churchill reveals 4 years of high BC and high NH_4^+ between 1933 and 1937, which correspond to years of low precipitation. And both the Alaska fire history and Bona-Churchill show 4 years of high fire activity during the 1940s. Interestingly, some of those years also correspond to El Niño years (1936, 1940–1941, and 1948, Figure 4c). In the later periods, summer temperatures are positively and significantly correlated with area burned (post-1950) and BC (post-1978). A cool period followed 1950 until ∼1977, when there were only three large fires in Alaska, and only 2 years of high BC or NH_4^+ during each decade (Figure 5). The 2 largest fire years of the 20th century in Alaska, 1957, 1969, occurred in El Niño years during this cool period. In addition, years of high BC or NH_4^+ also occurred during El Niño years 1965, 1969, and 1972 within this cool period.

In summary, 14 large fires in Alaska and 13 high BC and NH_4^+ occurred in a timespan of ∼50 years between the 1930s and 1980, several of which occurred during dry years and during El Niño years. This changed after 1984 when 6 large fire years in Alaska and 9 years of high BC or NH_4^+ years occurred in a much shorter timespan (∼20 years) between 1980 and 2001 during El Niño years and when precipitation was "normal" or "below normal," but temperatures were "above average." Likewise, 9 large fire years occurred in Alaska between 2001 and 2019 (Figure 4a), including the largest fire in 2004, which was the driest and warmest year on record (Figure 4b). Several of these 21st century large fire years occurred during low and normal precipitation years when temperatures were 1–1.5°C higher than during the 1930–1970s period (Figure 4b). These observations suggest that warmer temperatures likely played a more important role in the high fire activity after the 1980s.

Finally, lightning activity, a key ignition of wildfires, has increased in Alaska since the 1980s and it is projected to increase in Alaska (Bieniek et al., 2020) and the Arctic due to continued warming (Holzworth et al., 2021). Thus, the 1990s increase in large fire years in Alaska and high BC or NH_4^+ years in the Bona-Churchill ice core likely result from increased availability of dry organic matter coupled with enhanced lightning activity. It appears that the effects of high temperatures outweigh those of precipitation and it has been projected that precipitation will need to increase by 7%–10% per 1°C to offset the temperature effects on Alaskan wildfires (Flannigan et al., 2016; Grabinski & McFarland, 2020).

3.3. Comparison With Other Regional Ice Core Records

To further understand the origin of BC and NH_4^+ we compare the Bona-Churchill ice core records with those from Aurora Peak, Mt. Logan, and Eclipse Icefield (Figure 1). Using three different ice cores from the Eclipse Icefield in the Yukon Territory of Canada, recovered in 1996 (1 core) and 2002 (2 cores), an NH_4^+ record was developed by Yalcin et al. (2006) and provided a 1000-year regional forest fire history for Alaska and Yukon. The Eclipse record shows high fire activity during the 1920–1940 period and 1980s, and low fire activity during the 1950s and 1960s, like Bona-Churchill which suggests common sources influenced both sites. Contrary to Eclipse and Bona-Churchill, the Mt. Logan NH_4^+ record showed the highest fire activity during the 1960s. Whitlow et al. (1994) concluded that in addition to regional forest fires, the Mt. Logan ice cores recorded more distant forest fires from Siberia due to its higher altitude (920 m higher than Bona-Churchill and 2,323 m higher than Eclipse; Whitlow et al., 1994; Yalcin et al., 2006).

Yalcin et al. (2006) used NH_4^+ concentration residuals in association with other proxies of biomass burning ($C_2O_4^{2-}$ and K^+) to identify fire events in Eclipse (the reader is directed to the original publications as only the NH_4^+ concentrations are shown here) and considered high fire years in Alaska as those when more than 530,000 ha burned (1.5 times the 1940–2002 average). Regardless of the various parameters used to identify large fires, 9 large Alaskan fires (1940, 1941, 1947, 1950, 1969, 1977, 1988, 1990, 1991) were identified in both the Bona-Churchill and Eclipse ice cores.
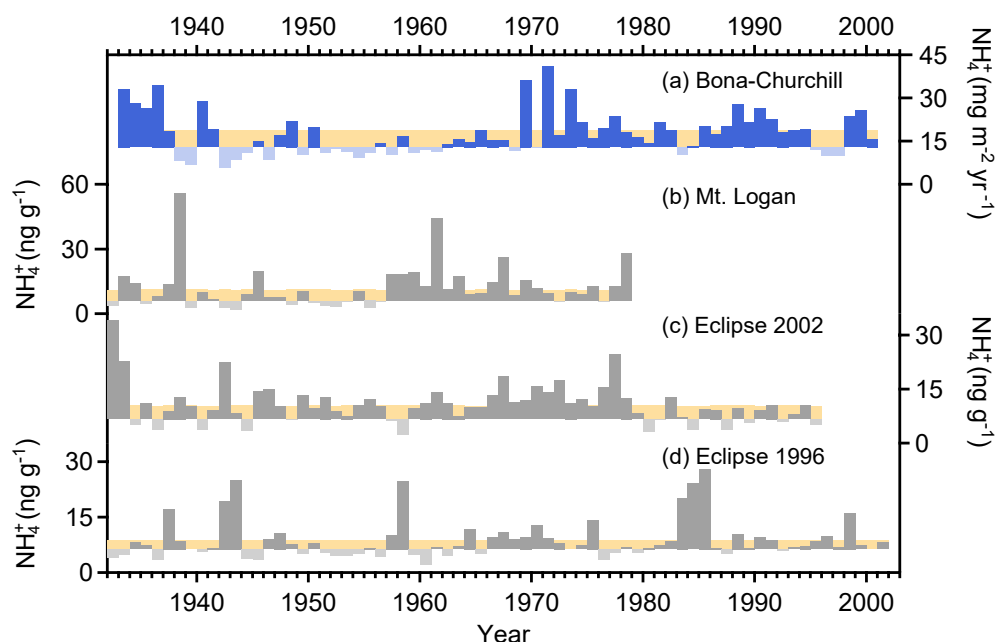
Figure 6. Ice core records of ammonium from (a) Bona-Churchill, (b) Mt. Logan (Whitlow et al., 1994), (c) Eclipse 2002 (Yalcin et al., 2006), and (d) Eclipse 1996 (Yalcin et al., 2006). The shaded areas in the records represent the middle percentile (33rd–66th percentile of their respective distribution) considered here as "normal".

The Eclipse ice cores recorded 36%–67% of large fire years in Alaska between 1940 and 2001 while Bona-Churchill recorded 67%. Yalcin et al. (2006) reported a 70% agreement among the three Eclipse cores except in the 1930s, 1970s, and 1980s, probably due to considerable spatial variability among the three Eclipse drilling sites due to drifting snow. This might explain why the records do not compare well among themselves or with the Bona-Churchill record (Figure 6). Likewise, Porter et al. (2019) found few similarities between the δ^{18}O record of Bona-Churchill and those of Mt. Logan and Eclipse likely due to the differences in altitude and topography.

Although the Aurora Peak ice core records are not continuous (Figures 7a–7c), some large fire years were identified. For example, there is a levoglucosan peak in 1947 that likely reflects the large 1947 Kenai fire season (also identified in the Bona-Churchill and the Eclipse ice cores). Levoglucosan also peaks in 1966, 1993, and 1999, the latter two of which correspond to years with large fires and high BC or NH$_4^+$ in Bona-Churchill. The vanillic acid concentration increased in 1973, and the BC and NH$_4^+$ concentrations increased in Bona-Churchill between 1971 and 1974, a period of low precipitation in Alaska. While 1973 is not considered a large fire year in Alaska, both the Aurora Peak and Bona-Churchill ice cores recorded a period of high fire activity in the region during the early 1970s. Contrary to the Eclipse and Mt. Logan ice core records, vanillic and dehydroabietic acids in the Aurora Peak ice core increased during the 1990s similar to BC from Bona Churchill, suggesting high biomass burning activity during this period when the number of large fires increased in Alaska (Figures 4 and 7). Thus, Aurora Peak, like Bona-Churchill, seems to have recorded regional fire activity during the 20th century.

The cluster analysis of air parcel trajectories shows that all four ice core sites are dominated by southerly flow (Figure S5 in Supporting Information S1). Moderate northwesterly flows from interior Alaska arrive at all four sites in the 3-day back trajectories clusters and northwesterly flows persist in the 5-day back trajectories clusters at three of the core sites, but do not reach Mt. Logan (Figure S5 in Supporting Information S1). The cluster analyses suggest that local emissions affect all four sites, while medium-range transport from interior Alaska affects Aurora Peak and Bona-Churchill most strongly, and Eclipse to a lesser extent. The differences among the flow patterns likely reflect the differences in the drill sites' inland location, local geography (topography), and altitude. Mt. Logan, the highest of the four sites, receives long-range air parcels from Siberia, which is consistent with previous findings (Whitlow et al., 1994). Aurora Peak, located furthest inland and at the lowest altitude (2,825 m asl), receives the strongest northwesterly flow from interior Alaska, followed by Bona-Churchill, which is located further inland than Eclipse and Mt. Logan but at a higher altitude than Aurora Peak. This likely explains
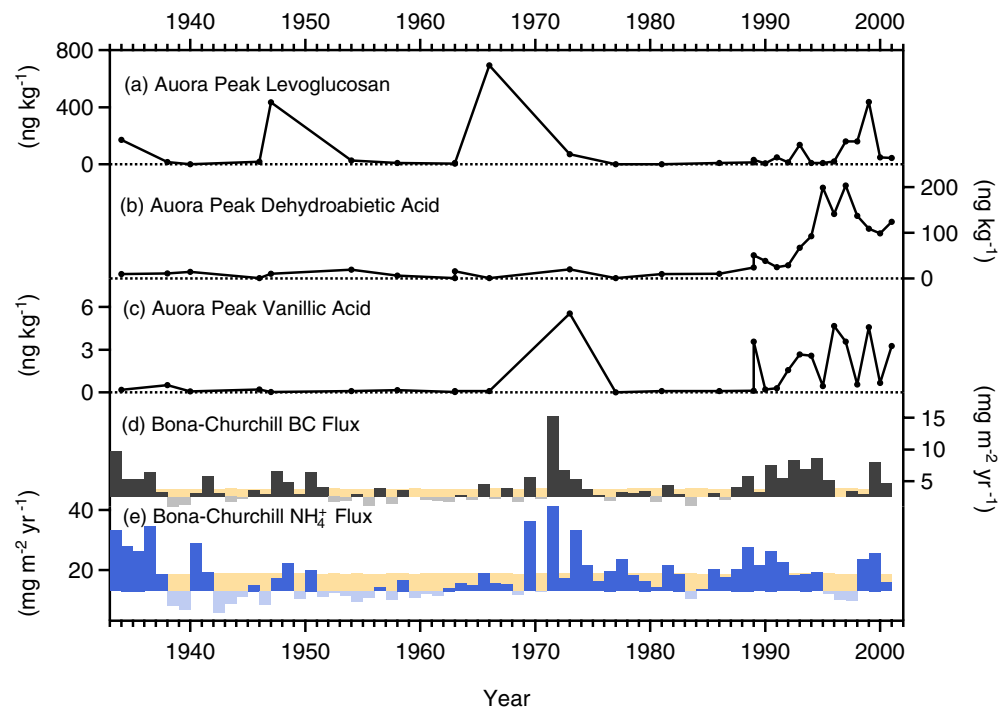
Figure 7. Comparison of concentrations of (a) levoglucosan, (b) dehydroabietic, and (c) vanillic acid in the Aurora peak ice core (Pokhrel et al., 2020) with the Bona-Churchill (d) black carbon, and (e) NH_4^+ fluxes between 1933 and 2002. The shaded areas in the Bona-Churchill records represent the middle (33rd–66th) percentile of the distribution which is considered here as "normal".

why the Bona-Churchill and Aurora Peak records show more similar trends, regardless of their different biomass burning proxies, and further confirms that BC and NH_4^+ at Bona-Churchill very likely originate from biomass burning and thus provide a record that reflects the fire history of Alaska.

4. Conclusions

An investigation of a continuous high-resolution ice core record of black carbon and ammonium (NH_4^+) from Bona-Churchill, southeast Alaska, demonstrates that this ice core provides a record of Alaskan forest fire activity between 1933 and 2001 that is consistent with the documented Alaskan fire history trends. Most of the high BC or NH_4^+ years in the Bona-Churchill ice core record occurred during El Niño events, similar to the large fire years in Alaska. Several of these years correspond to periods of low precipitation between 1939 and 1980s and strongly suggest that precipitation played an important role modulating fire activity in Alaska before 1978. However, after 1984, the frequency of large fires years in Alaska increased as reflected in the Bona-Churchill core despite "normal" precipitation levels, likely due to rising air temperatures, a trend that has continued into the 21st century.

Arctic ice core records of BC from Greenland and Svalbard have been overwhelmed by anthropogenic emissions (McConnell et al., 2007; Ruppel et al., 2014). However, this is not the case in Alaska. The Bona-Churchill ice field, similar to those on Eclipse, Mt. Logan, and Aurora Peak, is a sink for biomass burning emission products. Bona-Churchill rises above the boreal forests of the Wrangell-St Elias Mountain range and is subjected to northwesterly flow from interior Alaska where most of the wildfires occur. Additionally, the dominant southerly airmasses that reach these sites do not originate from industrialized areas, and thus do not affect the BC concentrations preserved on Bona-Churchill. Extension of the BC record to the bottom of the Bona-Churchill ice core (B-Ch1) could potentially provide a longer, continuous, and high-resolution record of forest fire and climate variability in a region where more information is required to identify the primary mechanisms driving Alaskan forest fires on multicentury time scales.

Conflict of Interest

The authors declare no conflicts of interest relevant to this study.

Data Availability Statement

The data presented in this work are archived at the NOAA's National Centers for Environmental Information for Paleoclimatology (https://www.ncdc.noaa.gov/paleo/study/35133).

References

AICC. (2020). *Alaska Interagency Coordination center: Alaska fire history chart with data*.

Anderson, R. S., Hallett, D. J., Berg, E., Jass, R. B., Toney, J. L., de Fontaine, C. S., & DeVolder, A. (2006). Holocene development of Boreal forests and fire regimes on the Kenai Lowlands of Alaska. *The Holocene*, *16*(6), 791–803. https://doi.org/10.1191/0959683606hol966rp

Barker, J. D., Kaspari, S., Gabrielli, P., Wegner, A., Beaudon, E., Sierra-Hernández, M. R., & Thompson, L. (2021). Drought-induced biomass burning as a source of black carbon to the Central Himalaya since 1781 CE as reconstructed from the Dasuopu Ice Core. *Atmospheric Chemistry and Physics*, *21*(7), 5615–5633. https://doi.org/10.5194/acp-21-5615-2021

Bieniek, P. A., Bhatt, U. S., York, A., Walsh, J. E., Lader, R., Strader, H., et al. (2020). Lightning variability in dynamically downscaled simulations of Alaska's present and future summer climate. *Journal of Applied Meteorology and Climatology*, *59*(6), 1139–1152. https://doi.org/10.1175/jamc-d-19-0209.1

Bieniek, P. A., Walsh, J. E., Thoman, R. L., & Bhatt, U. S. (2014). Using climate divisions to analyze variations and trends in Alaska temperature and precipitation. *Journal of Climate*, *27*(8), 2800–2818. https://doi.org/10.1175/jcli-d-13-00342.1

Bisiaux, M. M., Edwards, R., McConnell, J. R., Curran, M. A. J., Van Ommen, T. D., Smith, A. M., et al. (2012). Changes in black carbon deposition to Antarctica from two high-resolution ice core records, 1850–2000 AD. *Atmospheric Chemistry and Physics*, *12*(9), 4107–4115. https://doi.org/10.5194/acp-12-4107-2012

Bond, T. C., Bhardwaj, E., Dong, R., Jogani, R., Jung, S., Roden, C., et al. (2007). Historical emissions of black and organic carbon aerosol from energy-related combustion, 1850-2000. *Global Biogeochemical Cycles*, *21*(2). https://doi.org/10.1029/2006GB002840

Bond, T. C., Doherty, S. J., Fahey, D. W., Forster, P. M., Berntsen, T., DeAngelo, B. J., et al. (2013). Bounding the role of black carbon in the climate system: A scientific assessment. *Journal of Geophysical Research: Atmospheres*, *118*(11), 5380–5552. https://doi.org/10.1002/jgrd.50171

Chapin, F. S., III, Trainor, S. F., Huntington, O., Lovecraft, A. L., Zavaleta, E., Natcher, D. C., et al. (2008). Increasing wildfire in Alaska's boreal forest: Pathways to potential solutions of a wicked problem. *BioScience*, *58*(6), 531–540. https://doi.org/10.1641/b580609

Cooke, W. F., Liousse, C., Cachier, H., & Feichter, J. (1999). Construction of a 1° × 1° fossil fuel emission data set for carbonaceous aerosol and implementation and radiative impact in the ECHAM4 model. *Journal of Geophysical Research: Atmospheres*, *104*(D18), 22137–22162. https://doi.org/10.1029/1999jd900187

Crippa, M., Guizzardi, D., Muntean, M., Schaaf, E., Dentener, F., van Aardenne, J. A., et al. (2018). Gridded emissions of air pollutants for the period 1970–2012 within EDGAR v4.3.2. *Earth System Science Data*, *10*(4), 1987–2013. https://doi.org/10.5194/essd-10-1987-2018

Crippa, M., Oreggioni, G., Guizzardi, D., Muntean, M., Schaaf, E., Lo Vullo, E., et al. (2019). *Fossil CO2 and GHG emissions of all world countries. 2019 Report*.

De Volder, A. (1999). *Fire and climate history of lowland black spruce forests* (p. 128). Kenai National Wildlife Refuge, Northern Arizona University.

DeWilde, L., & Chapin, F. S., III (2006). Human impacts on the fire regime of interior Alaska: Interactions among fuels, ignition sources, and fire suppression. *Ecosystems*, *9*(8), 1342–1353. https://doi.org/10.1007/s10021-006-0095-0

Dey, P. (2021). *Sequential Mann Kendall test. MATLAB Central file Exchange*.

Drury, S. A., & Grissom, P. J. (2008). Fire history and fire management implications in the Yukon Flats National Wildlife Refuge, interior Alaska. *Forest Ecology and Management*, *256*, 304–312. https://doi.org/10.1016/j.foreco.2008.04.040

Duffy, P. A., Walsh, J. E., Graham, J. M., Mann, D. H., & Rupp, T. S. (2005). Impacts of large-scale atmospheric–ocean variability on Alaskan fire season severity. *Ecological Applications*, *15*(4), 1317–1330. https://doi.org/10.1890/04-0739

EDGARv5.0. (2020). European Commission, Joint Research Centre (EC-JRC)/Netherlands environmental assessment agency (PBL). Emissions database for global atmospheric Research (EDGAR), release EDGAR v5.0 (1970 – 2015). Emission grid maps 0.1degree x 0.1degree, edited, Retrieved from https://data.europa.eu/doi/10.2904/JRC_DATASET_EDGAR

EIA. (2019). *U.S. Energy information Administration. State energy consumption estimates 1960 through 2017*.

Fernandes, S. M., Trautmann, N. M., Streets, D. G., Roden, C. A., & Bond, T. C. (2007). Global Biofuel Use, 1850–2000, *Global Biogeochemical Cycles* (Vol. 21, p. GB2019). https://doi.org/10.1029/2006GB002836

Flannigan, M. D., Wotton, B. M., Marshall, G. A., de Groot, W. J., Johnston, J., Jurko, N., & Cantin, A. S. (2016). Fuel moisture sensitivity to temperature and precipitation: Climate change implications. *Climatic Change*, *134*(1), 59–71. https://doi.org/10.1007/s10584-015-1521-0

Gelaro, R., McCarty, W., Suárez, M. J., Todling, R., Molod, A., Takacs, L., et al. (2017). The modern-era retrospective analysis for research and applications, version 2 (MERRA-2). *Journal of Climate*, *30*(14), 5419–5454. https://doi.org/10.1175/jcli-d-16-0758.1

Grabinski, Z., & McFarland, H. R. (2020). Alaska's changing wildfire environment [outreach booklet], Alaska Fire Science Consortium, International Arctic Research Center. University of Alaska Fairbanks.

Greet, J., Valerio, P., Diego, G., & Marilena, M. (2013). Global emission inventories in the Emission Database for Global Atmospheric Research (EDGAR)@ Manual (I) I. Gridding: EDGAR emissions distribution on global gridmaps.

Hayasaka, H., Tanaka, H. L., & Bieniek, P. A. (2016). Synoptic-scale fire weather conditions in Alaska. *Polar Science*, *10*(3), 217–226. https://doi.org/10.1016/j.polar.2016.05.001

Hegg, D. A., Warren, S. G., Grenfell, T. C., Sarah, J. D., & Clarke, A. D. (2010). Sources of light-absorbing aerosol in arctic snow and their seasonal variation. *Atmospheric Chemistry and Physics*, *10*(22), 10923–10938. https://doi.org/10.5194/acp-10-10923-2010

Hess, J. C., Scott, C. A., Hufford, G. L., & Fleming, M. D. (2001). El Niño and its impact on fire weather conditions in Alaska. *International Journal of Wildland Fire*, *10*(1), 1–13. https://doi.org/10.1071/WF01007

Holzworth, R. H., Brundell, J. B., McCarthy, M. P., Jacobson, A. R., Rodger, C. J., & Anderson, T. S. (2021). Lightning in the Arctic. *Geophysical Research Letters*, *48*, e2020GL091366. https://doi.org/10.1029/2020GL091366

Hu, F. S., Higuera, P. E., Duffy, P., Chipman, M. L., Rocha, A. V., Young, A. M., et al. (2015). Arctic tundra fires: Natural variability and responses to climate change. *Frontiers in Ecology and the Environment*, *13*(7), 369–377. https://doi.org/10.1890/150063

Kalnay, E., Kanamitsu, M., Kistler, R., Collins, W., Deaven, D., Gandin, L., et al. (1996). The NCEP/NCAR 40-year reanalysis project. *Bulletin of the American Meteorological Society*, *77*(3), 4372–4471. https://doi.org/10.1175/1520-0477(1996)077<0437:tnyrp>2.0.co;2

Kasischke, E. S., Amiro, B. D., Barger, N. N., French, N. H. F., Goetz, S. J., Grosse, G., et al. (2013). Impacts of disturbance on the terrestrial carbon budget of North America. *Journal of Geophysical Research: Biogeosciences*, *118*(1), 303–316. https://doi.org/10.1002/jgrg.20027

Kasischke, E. S., Verbyla, D. L., Rupp, T. S., McGuire, A. D., Murphy, K. A., Jandt, R., et al. (2010). Alaska's changing fire regime — implications for the vulnerability of its boreal forests. *Canadian Journal of Forest Research*, *40*(7), 1313–1324. https://doi.org/10.1139/x10-098

Kasischke, E. S., Williams, D., & Barry, D. (2002). Analysis of the patterns of large fires in the boreal forest region of Alaska. *International Journal of Wildland Fire*, *11*(2), 131–144. https://doi.org/10.1071/WF02023

Kaspari, S. D., Pittenger, D., Jenk, T. M., Morgenstern, U., Schwikowski, M., Buenning, N., & Stott, L. (2020). Twentieth century black carbon and dust deposition on south Cascade glacier, Washington state, USA, as reconstructed from a 158-m-long ice core. *Journal of Geophysical Research: Atmospheres*, *125*(11), e2019JD031126. https://doi.org/10.1029/2019JD031126

Kaspari, S. D., Schwikowski, M., Gysel, M., Flanner, M. G., Kang, S., Hou, S., & Mayewski, P. A. (2011). Recent increase in black carbon concentrations from a Mt. Everest ice core spanning 1860–2000 AD. *Geophysical Research Letters*, *38*(4). https://doi.org/10.1029/2010GL046096

Keegan, K. M., Albert, M. R., McConnell, J. R., & Baker, I. (2014). Climate change and forest fires synergistically drive widespread melt events of the Greenland Ice Sheet. *Proceedings of the National Academy of Sciences*, *111*(22), 7964–7967. https://doi.org/10.1073/pnas.1405397111

Legrand, M., McConnell, J., Fischer, H., Wolff, E. W., Preunkert, S., Arienzo, M., et al. (2016). Boreal fire records in northern Hemisphere ice cores: A review. *Climate of the Past*, *12*(10), 2033–2059. https://doi.org/10.5194/cp-12-2033-2016

Lim, S., Faïn, X., Ginot, P., Mikhalenko, V., Kutuzov, S., Paris, J. D., et al. (2017). Black carbon variability since preindustrial times in the eastern part of Europe reconstructed from Mt. Elbrus, Caucasus, ice cores. *Atmospheric Chemistry and Physics*, *17*(5), 3489–3505. https://doi.org/10.5194/acp-17-3489-2017

Lund, M. T., & Berntsen, T. (2012). Parameterization of black carbon aging in the OsloCTM2 and implications for regional transport to the Arctic. *Atmospheric Chemistry and Physics*, *12*(15), 6999–7014. https://doi.org/10.5194/acp-12-6999-2012

Lund, M. T., Berntsen, T. K., & Samset, B. H. (2017). Sensitivity of black carbon concentrations and climate impact to aging and scavenging in OsloCTM2–M7. *Atmospheric Chemistry and Physics*, *17*(9), 6003–6022. https://doi.org/10.5194/acp-17-6003-2017

Macias Fauria, M., & Johnson, E. A. (2008). Climate and wildfires in the North American boreal forest. *Philosophical Transactions of the Royal Society of London B Biological Sciences*, *363*(1501), 2317–2329. https://doi.org/10.1098/rstb.2007.2202

McConnell, J. R., Edwards, R., Kok, G. L., Flanner, M. G., Zender, C. S., Saltzman, E. S., et al. (2007). 20th-Century industrial black carbon emissions altered Arctic climate forcing. *Science*, *317*(5843), 1381–1384. https://doi.org/10.1126/science.1144856

Menking, J. A. (2013). *Black carbon measurements of snow and ice using the single particle soot photometer: Method development and an AD 1852–1999 record of atmospheric black carbon from a Mount Logan ice core* (p. 200). Master thesisCentral Washington University.

Nguyen, P.-L., Min, S.-K., & Kim, Y.-H. (2021). Combined impacts of the El Niño-Southern Oscillation and Pacific Decadal Oscillation on global droughts assessed using the standardized precipitation evapotranspiration index. *International Journal of Climatology*, *41*(S1), E1645–E1662. https://doi.org/10.1002/joc.6796

Niranjan, R., & Thakur, A. K. (2017). The toxicological mechanisms of environmental soot (black carbon) and carbon black: Focus on oxidative stress and inflammatory pathways. *Frontiers in Immunology*, *8*(763). https://doi.org/10.3389/fimmu.2017.00763

NOAA. (2020a). *National Centers for environmental information, climate at a glance: Statewide Mapping*.

NOAA. (2020b). *Niño 3.4*. Standard PSL Format.

Osmont, D., Wendl, I. A., Schmidely, L., Sigl, M., Vega, C. P., Isaksson, E., & Schwikowski, M. (2018). An 800-year high-resolution black carbon ice core record from Lomonosovfonna, Svalbard. *Atmospheric Chemistry and Physics*, *18*(17), 12777–12795. https://doi.org/10.5194/acp-18-12777-2018

Papineau, J. M. (2001). Wintertime temperature anomalies in Alaska correlated with ENSO and PDO. *International Journal of Climatology*, *21*(13), 1577–1592. https://doi.org/10.1002/joc.686

Partain, J. L., Alden, S., Bhatt, U. S., Bieniek, P. A., Brettschneider, B. R., Lader, R. T., et al. (2016). An assessment of the role of anthropogenic climate change in the Alaska fire season of 2015. *Bulletin of the American Meteorological Society*, *97*(12), S14–S18. https://doi.org/10.1175/bams-d-16-0149.1

Pokhrel, A., Kawamura, K., Kunwar, B., Ono, K., Tsushima, A., Seki, O., et al. (2020). Ice core records of levoglucosan and dehydroabietic and vanillic acids from Aurora peak in Alaska since the 1660s: A proxy signal of biomass-burning activities in the north Pacific Rim. *Atmospheric Chemistry and Physics*, *20*(1), 597–612. https://doi.org/10.5194/acp-20-597-2020

Porter, S. E., Mosley-Thompson, E., & Thompson, L. G. (2019). Ice core $\delta^{18}O$ record linked to western Arctic sea ice variability. *Journal of Geophysical Research: Atmospheres*, *124*(20), 10784–10801. https://doi.org/10.1029/2019jd031023

Qi, L., & Wang, S. (2019a). Fossil fuel combustion and biomass burning sources of global black carbon from GEOS-Chem simulation and carbon isotope measurements. *Atmospheric Chemistry and Physics*, *19*(17), 11545–11557. https://doi.org/10.5194/acp-19-11545-2019

Qi, L., & Wang, S. (2019b). Sources of black carbon in the atmosphere and in snow in the Arctic. *The Science of the Total Environment*, *691*, 442–454. https://doi.org/10.1016/j.scitotenv.2019.07.073

Randles, C. A., da Silva, A. M., Buchard, V., Colarco, P. R., Darmenov, A., Govindaraju, R., et al. (2017). The MERRA-2 aerosol reanalysis, 1980 onward. Part I: System description and data assimilation evaluation. *Journal of Climate*, *30*(17), 6823–6850. https://doi.org/10.1175/jcli-d-16-0609.1

Randles, C. A., Silva, A. M. d., Buchard, V., Darmenov, A., Colarco, P. R., Aquila, V., et al. (2016). *The MERRA-2 Aerosol Assimilation*. Technical Report Series on Global Modeling and Data Assimilation (Vol. 45).

Rayner, N. A., Parker, D. E., Horton, E. B., Folland, C. K., Alexander, L. V., Rowell, D. P., et al. (2003). Global analyses of sea surface temperature, sea ice, and night marine air temperature since the late nineteenth century, *Journal of Geophysical Research*, *108*(D14), 4407. https://doi.org/10.1029/2002JD002670

Reid, C. E., Brauer, M., Johnston, F. H., Jerrett, M., Balmes, J. R., & Elliott, C. T. (2016). Critical review of health impacts of wildfire smoke exposure. *Environmental Health Perspectives*, *124*(9), 1334–1343. https://doi.org/10.1289/ehp.1409277

Ruppel, M. M., Isaksson, E., Ström, J., Beaudon, E., Svensson, J., Pedersen, C. A., & Korhola, A. (2014). Increase in elemental carbon values between 1970 and 2004 observed in a 300-year ice core from Holtedahlfonna (Svalbard). *Atmospheric Chemistry and Physics*, *14*(20), 11447–11460. https://doi.org/10.5194/acp-14-11447-2014

Schwarz, J. P., Doherty, S. J., Li, F., Ruggiero, S. T., Tanner, C. E., Perring, A. E., et al. (2012). Assessing single particle soot photometer and integrating sphere/integrating sandwich spectrophotometer measurement techniques for quantifying black carbon concentration in snow. *Atmospheric Measurement Techniques*, *5*(11), 2581–2592. https://doi.org/10.5194/amt-5-2581-2012

Schwarz, J. P., Gao, R. S., Fahey, D. W., Thomson, D. S., Watts, L. A., Wilson, J. C., et al. (2006). Single-particle measurements of midlatitude black carbon and light-scattering aerosols from the boundary layer to the lower stratosphere. *Journal of Geophysical Research: Atmospheres*, *111*(D16). https://doi.org/10.1029/2006jd007076

Sigl, M., Abram, N. J., Gabrieli, J., Jenk, T. M., Osmont, D., & Schwikowski, M. (2018). 19th century glacier retreat in the Alps preceded the emergence of industrial black carbon deposition on high-alpine glaciers. *The Cryosphere*, *12*, 3311–3331. https://doi.org/10.5194/tc-12-3311-2018

Todd, S. K., & Jewkes, H. A. (2006). *Wildland fire in Alaska: A history of organized fire suppression and management in the Last Frontier*.

Urmann, D. (2009). *Decadal scale climate variability during the Last Millennium as recorded by the Bona Churchill and Quelccaya ice cores, Doctoral Dissertation thesis*. The Ohio State University.

Wang, M., Xu, B., Kaspari, S. D., Gleixner, G., Schwab, V. F., Zhao, H., et al. (2015). Century-long record of black carbon in an ice core from the Eastern Pamirs: Estimated contributions from biomass burning. *Atmospheric Environment*, *115*, 79–88. https://doi.org/10.1016/j.atmosenv.2015.05.034

Wendl, I. A., Menking, J. A., Färber, R., Gysel, M., Kaspari, S. D., Laborde, M. J. G., & Schwikowski, M. (2014). Optimized method for black carbon analysis in ice and snow using the Single Particle Soot Photometer. *Atmospheric Measurement Techniques*, *7*(8), 2667–2681. https://doi.org/10.5194/amt-7-2667-2014

Whitlow, S., Mayewski, P., Dibb, J., Holdsworth, G., & Twickler, M. (1994). An ice-core-based record of biomass burning in the Arctic and Subarctic, 1750–1980. *Tellus B: Chemical and Physical Meteorology*, *46*(3), 234–342. https://doi.org/10.3402/tellusb.v46i3.15794

Winiger, P., Barrett, T. E., Sheesley, R. J., Huang, L., Sharma, S., Barrie, L. A., et al. (2019). Source apportionment of circum-Arctic atmospheric black carbon from isotopes and modeling. *Science Advances*, *5*(2), eaau8052. https://doi.org/10.1126/sciadv.aau8052

Yalcin, K., Wake, C. P., Kreutz, K. J., & Whitlow, S. I. (2006). A 1000-yr record of forest fire activity from Eclipse Icefield, Yukon, Canada. *The Holocene*, *16*(2), 200–209. https://doi.org/10.1191/0959683606hl920rp

York, A., Bhatt, U. S., Gargulinski, E., Grabinski, Z., Jain, P., Soja, A., et al. (2020). *Arctic report card 2020: Wildland fire in high northern latitudes*. https://doi.org/10.25923/2gef-3964

Young, A. M., Higuera, P. E., Duffy, P. A., & Hu, F. S. (2017). Climatic thresholds shape northern high-latitude fire regimes and imply vulnerability to future climate change. *Ecography*, *40*(5), 606–617. https://doi.org/10.1111/ecog.02205

Zdanowicz, C. M., Proemse, B. C., Edwards, R., Feiteng, W., Hogan, C. M., Kinnard, C., & Fisher, D. (2018). Historical black carbon deposition in the Canadian high Arctic: A >250-year long ice-core record from Devon Island. *Atmospheric Chemistry and Physics*, *18*(16), 12345–12361. https://doi.org/10.5194/acp-18-12345-2018

Zhang, Y., Li, M., Cheng, Y., Geng, G., Hong, C., Li, H., et al. (2019). Modeling the aging process of black carbon during atmospheric transport using a new approach: A case study in Beijing. *Atmospheric Chemistry and Physics*, *19*(14), 9663–9680. https://doi.org/10.5194/acp-19-9663-2019